Estimation of Bed Shear Stress using Turbulent Kinetic Energy in Three-dimensional Complex Flow Fields around an Obstruction in a Coarse Bed River

Jun Seon lee[1] and seung ho hong[1]

[1]West Virginia University

November 24, 2022

Abstract

Erosion, transport, and deposition of a river-bed has attracted attentions from various disciplines. To understand those issues, bed shear stress should be evaluated first. However, calculating bed shear stress with existing formulas have certain limitations because uniform and/or gradually-varied flow was assumed in their studies, which is hardly found in an actual river. Therefore, direct applying them into three-dimensional complex flow field, such as flow around a bridge obstruction or a large-rock, is questionable. Thus, laboratory experiment was conducted in a flume and the results were used to suggest a method of bed shear stress estimation in the complex flow field. To generate the complex flow field, three different width of obstruction was constructed and installed in one side of the flume. Water depth, velocities, and turbulence intensities were measured, and the measurements were used as input variables of four different widely used existing shear stress formulas for their evaluation. Then, the effects of local turbulence on the shear stress were discussed in terms of Reynolds stress and turbulent kinetic energy (TKE) measured under a wide range of flow variables. Based on the findings, bed shear stress can be estimated with an empirical correction factor for the local turbulence around the obstruction where elevated region of bed shear stress is found, and the experimental result shows that the correction factor is function of the value of flow contraction ratio. The results are expected to be a useful outcome to understand the mechanism of geomorphological change under rapidly-varied non-uniform flow.

Estimation of Bed Shear Stress using Turbulent Kinetic Energy in Three-dimensional Complex Flow Fields around an Obstruction in a Coarse Bed River

Jun Seon Lee[1], and Seung Ho Hong[2]

[1]Graduate student, Department of Civil and Environmental Engineering, West Virginia University, 1306 Evansdale Drive, Morgantown WV 26506, USA.

[2]Assistant Professor, Department of Civil and Environmental Engineering, West Virginia University, 1306 Evansdale Drive, Morgantown WV 26506, USA.

Corresponding author: Seung Ho Hong (sehong@mail.wvu.edu)

Key Points:

- Reproduce complex three dimensional flow fields in the laboratory to explore the effect of local turbulence on the bed shear stress
- Finding relationship between shear stress and turbulent kinetic energy via empirical coefficient which has direct function with flow contraction ratio
- Suggesting a surrogate method of estimating bed shear stress using turbulent kinetic energy

Abstract

Erosion, transport, and deposition of a river-bed has attracted attentions from various disciplines. To understand those issues, bed shear stress should be evaluated first. However, calculating bed shear stress with existing formulas have certain limitations because uniform and/or gradually-varied flow was assumed in their studies, which is hardly found in an actual river. Therefore, direct applying them into three-dimensional complex flow field, such as flow around a bridge obstruction or a large-rock, is questionable. Thus, laboratory experiment was conducted in a flume and the results were used to suggest a method of bed shear stress estimation in the complex flow field. To generate the complex flow field, three different width of obstruction was constructed and installed in one side of the flume. Water depth, velocities, and turbulence intensities were measured, and the measurements were used as input variables of four different widely used existing shear stress formulas for their evaluation. Then, the effects of local turbulence on the shear stress were discussed in terms of Reynolds stress and turbulent kinetic energy (TKE) measured under a wide range of flow variables. Based on the findings, bed shear stress can be estimated with an empirical correction factor for the local turbulence around the obstruction where elevated region of bed shear stress is found, and the experimental result shows that the correction factor is function of the value of flow contraction ratio. The results are expected to be a useful outcome to understand the mechanism of geomorphological change under rapidly-varied non-uniform flow.

1 Introduction

1.1 Background

To understand the mechanisms of bed material's movement in a river including erosion, transport, and deposition (Landers & Sturm, 2013), hydrodynamic drag forces induced by flowing water, also called shear stress, should be compared with the geotechnical/gravitational/interparticle electrochemical resistance, which is critical shear stress, of the materials (Buscombe & Conley, 2012; Choo et al., 2020; Shvidchenko et al., 2001). In addition to the force by those natural phenomena in one-dimensional flow, flow obstructions by a large rock or human-made infrastructure generate additional macro-turbulence around the obstructions, causing higher shear stress locally and making the problem of sedimentation more difficult to understand. The higher shear stress lead to change of bed-morphology and, sometimes, failure of hydraulic infrastructure by scouring of their foundation. Furthermore, understanding within the recirculation region behind the structure with respect to the magnitude of shear stress is also important because the sediment deposition within the region can encourage vegetation growth (Etminan et al., 2018), providing further stabilization of the banks as well as habitat for fish and other aquatic species (Bouteiller & Venditti, 2015; Yang et al., 2015). Accordingly, bed shear stress has been used intensively to analyze drag force related to the bed roughness as in bed-load transport (Cheng et al., 2004; Einstein, 1942; Parker & Klingeman, 1982; Monsalve & Yager 2017; Mueller et al., 2005; Shield, 1936), deposition, bedform and channel change (Monteith & Pender 2005; Sukhodolov, 2012; Wilcock, 1996,) as well as sediment transport around natural and/or man-made infrastructure (Hong & Abid, 2019; Hong & Lee, 2018; Hong et al., 2015; Jeon et al., 2018; Kang et al., 2016; Lee & Hong, 2019; Petit, 1987). In addition to the shear stress related to the bed roughness, for flow through compound shape of open channel, including interface between floodplain flow and main-channel flow as wetted perimeter for the calculation of total discharge has also been discussed by several researchers (Knight & Demetrio, 1983; Myers, 1978; Myers & Lyness, 1997; Shiono & Knight, 1991; Wormleaton & Hadjipanos, 1985) because the effect of shear stress between the faster moving main-channel flow and the floodplain flow result in smaller value of total discharge than the value by simply adding the discharges of the main channel and flood-plains. As explained in the studies conducted by several other researchers, the topic of shear stress has been studied in various disciplines to understand the underpinning mechanisms of their own physical process, but still remaining challenging problems is “How to calculate shear stress more accurately?”.

Prediction of shear stress has been focused in various ways, but there are two major limitations. One of the limitations is that there are only a few studies regarding rapidly-varied and/or non-uniform flow which is common flow types in the field that can causes rapid change of river bed during extreme hydrologic conditions under current climate change. Most of existing studies for shear stress have been conducted under a gradually-varied flow and/or uniform flow (Cardoso et al., 1991; Kironoto & Graf, 1995; Nezu & Nakagawa, 1993; Nezu et al., 1997; Tu & Graf, 1993; Song & Chiew, 2001; Yang, 2005). Another limitation of many of current shear stress formulas is that they used one-dimensional turbulence measurements as input values, such as measured by using Prantl-Pitot tubes and shear plate (Ahmed & Rajaratnam, 1998; Rankin & Hires, 2000; Shamloo et al., 2001). Therefore, characteristic of three-dimensional turbulent on shear stress could not be represented correctly with those measurements’ devices. More recently, several research attempts including Biron et al. (2004), Duan (2009), Johnson and Cowen (2017) and Sime et al. (2007) were made to estimate shear stress using flow variables measured by more precise measuring devices, but only relative amount of shear stress, not absolute value, was calculated by using current formulas and compared with the bed contours in their experiment.

Thus, in this study, to overcome the limitations explained above, experiments were carried out with an artificial shape of obstruction structure in the laboratory for the purpose of analyzing shear stress in the complex flow which can be easily found in a field. Three different size of artificial structure were built in the flume to find the effect of local turbulent structure through the flow contraction caused by reduced flow area on the shear stress. With the measured hydraulic variables including velocities, water depths, and turbulent quantities, shear stress is estimated with using various existing shear stress formulas in the approach and the test section where the structure was installed. With the findings, parametric coefficient is suggested for the calculation of bed shear stress which account for the local turbulence effect around the different size of the obstruction where elevated value of shear stress was found. Furthermore, characteristics of bed shear stress in the approach and the rapidly-varied flow area are quantitatively explained.

1.2 Bed shear stress equation

Usually, bed shear stress formula can be categorized by required data set for the calculation: 1) water depth, 2) shear velocity, 3) Reynolds stress, and 4) turbulent kinetic energy (TKE). Based on the data set, corresponding four widely used bed shear stress equations were selected in this study and used for comparing results of estimated bed shear stress. Detailed descriptions of selected equations are explained below.

1.2.1 Shear stress equation using water depth

Bed shear stress equation using water depth is the most basic/simple and, thus, can be found in many fundamental fluid mechanics and open channel textbook (e.g., Chow, 1959; Sturm, 2010).

In steady and uniform flow, the shear stress equation using water depth can be derived by force balance as follows,

$$\tau_b = \gamma R S_0 \qquad \text{Eq. (1)}$$

where, τ_b: bed shear stress, γ: specific weight, R: hydraulic radius, and S_0: bed slope. Eq. (1) is simple and widely used to calculate bed shear stress by engineering and geology communities because hydraulic radius, which is function of water depth and shape of cross-section, is only required variable when the bed slope is given. However, too much simplified assumption, such as steady-uniform flow, results in larger bed shear stress than the actual value because they ignored the effect of friction with respect to the different bed materials (Nezu & Nakagawa, 1993). Furthermore, the method is not suitable for local and small-scale evaluation such as for around a large rock and a bridge (Biron et al., 2004).

1.2.2 Shear stress equation using shear velocity

Shear stress can also be estimated by using shear velocity. Based on the mixing length theory of Prandtl (1875-1973), velocity fluctuation can be described with the velocity gradient and a specific length scale (mixing length) which is direct proportion with the von Karman's constant ($\kappa = 0.4$ in the gradually $-$ varied flow) and distance from the bed. By the concept, Ligrani and Moffat (1986) suggested following equation that can be used to estimate shear velocity.

$$\frac{u(z)}{u_*} = \frac{1}{\kappa}\ln\left(\frac{z+z_0}{k_s}\right) + B_R \qquad \text{Eq. (2)}$$

where, u: point velocity in flow direction, z: distance from the bed, u_*: shear velocity, κ: von Karman's constant, z_0: displacement height, κ_s: grain roughness element, and B_R: constant value by roughness-geometry characteristics that vary with roughness Reynolds number. Therefore, when the data for vertical velocity profile and grain roughness element are available, shear velocity can be calculated, and the bed shear stress is estimated by using following formula.

$$\tau_b = \rho (u_*)^2 = \rho\left(\frac{u(z)}{\frac{1}{\kappa}\ln\left(\frac{z+z_0}{k_s}\right)+B_R}\right)^2 \qquad \text{Eq. (3)}$$

where, ρ: water density. Eq. (3) is also simple and widely used for the calculation of bed shear stress because they only required vertical velocity profile and bed material's information. However, representative feature of Eq. (3) is that Eq. (3) can only be adaptable when the measured vertical velocity profile follows logarithmic function that may not actually occur in highly non-uniform and unsteady flow. Furthermore, as the vertical velocity profile is sensitively affected by the bed roughness, the results from Eq. (3) shows also larger value than the actual shear stress in coarse bed materials (Biron et al., 2004; Rowinski et al., 2005; Smart, 1999).

1.2.3 Shear stress equation using Reynolds stress

Reynolds stress is considered as one of the most important findings in turbulent flow and can be obtained from averaging of Navier-Stokes equation for incompressible flow (Kundu et al., 2015). As shown in Eq. (4), the equation includes three stress components that are mean pressure stress, mean viscous stress, and Reynolds stress,

$$\frac{\partial \overline{u_i}}{\partial t} + \overline{u_j}\frac{\partial \overline{u_i}}{\partial p_j} = \frac{1}{\rho}\frac{\partial}{\partial x_j}\left\{ \underbrace{-\bar{P}\delta_{ij}}_{\text{Mean pressure stress}} + \underbrace{\mu\left(\frac{\partial \overline{u_i}}{\partial p_j} + \frac{\partial \overline{u_j}}{\partial p_i}\right)}_{\text{Mean viscous stress}} - \underbrace{\rho\overline{u'_i u'_j}}_{\text{Reynolds stress}} \right\} \quad \text{Eq. (4)}$$

where, $\bar{P}$: Mean pressure, $\bar{u}$: mean velocity, i, j: the Cartesian components of vectors and tensors, t: time, p: flow direction, μ: viscosity, δ_{ij}: Kronecker delta.

Among the stress components in Eq. (4), shear stress is related with Reynolds stress tensor and viscous stress tensor. However, because the effect of viscosity in turbulent flow can be negligible, Reynolds stress ($\overline{u'v'}$, $\overline{u'w'}$, $\overline{v'w'}$) along the three physical planes (*xy*, *xz*, *yz* plane), where u', v' and w' are the velocity fluctuations of the streamwise (x), lateral (y) and vertical (z) components and upper bar denotes an average, are a component of stress tensor that can directly represent turbulent shear stress. For the validations, Nezu and Nakagawa (1993) conducted experiments using a straight-rectangular flume and showed that the measurement of vertical profile of Reynolds stress ($\overline{u'w'}$) shows good agreement with shear stress profile calculated by using Eq.(4). In their comparison, they could not consider other two components of Reynolds stress ($\overline{u'v'}$, $\overline{v'w'}$) because, in their experiment, the value of $\overline{u'v'}$ and $\overline{v'w'}$ shows negligible in their one dimensional experimental flow set-up. However, in the rapidly-varied flow or complex three-dimensional flow, all three components of Reynolds stress should be considered for predicting shear stress. Thus, Dey and Barbuiya (2005) used the shear stress equation and estimated components of bed shear stress in the flow direction (τ_{bx}) and lateral direction (τ_{by}) together with the concept of momentum flux (Mathieu & Scott, 2000) and suggested shear stress (τ_b) equation as follows.

$$\tau_{bx} = \overline{u'v'} + \overline{w'u'} \quad \text{Eq. (5)}$$

$$\tau_{by} = \overline{u'v'} + \overline{w'v'} \quad \text{Eq. (6)}$$

$$\tau_b = \rho((\overline{u'v'} + \overline{w'u'})^2 + (\overline{u'v'} + \overline{w'v'})^2)^{0.5} \quad \text{Eq. (7)}$$

Later, Duan (2009) applied Eq. (7) to the flow around spur dike on the sand bed to calculate bed shear stress and the result shows similar patterns with spatial distributions of scour contours. Thus, Reynolds stress has been considered as one of the most reliable method estimating bed shear stress, if velocity fluctuations can be measured accurately using precise measuring devices such as Acoustic Doppler Velocimetry (ADV), Laser Doppler Velocimetry (LDV), and Particle Image Velocimetry (PIV) (Nezu & Rodi, 1986; Nezu et al., 1997).

1.2.4 Shear stress equation using TKE

TKE consists of turbulent strength in three directions and is used to define total strength of turbulence within a region. The derivation of shear stress equation using TKE was originated from studies by Galperin et al. (1988) and Soulsby and Dyer (1981) that shows linear relationship between Reynolds stress and TKE. Based on the findings, an empirical coefficient was represented for oceanography studies, and defined as 0.19 (Soulsby & Dyer, 1981; Stapleton & Huntley, 1995). And the bed shear stress equation using TKE is derived as follows,

$$\tau_b = 0.19\rho k \qquad \text{Eq. (8)}$$

where, constant value (=0.19): empirical coefficient determined by the oceanography studies, k: value of turbulent kinetic energy (TKE) $(= 0.5(u'^2 + v'^2 + w'^2))$. The increase amount of turbulence in certain flow region provide additional energy to create local elevation of the shear stress and the value of TKE is a key parameter to account for the impact of the local turbulence energy generated by the vortex structure and separated shear layer (Ge et al., 2005; Lacey & Rennie, 2012, and Lefebvre et al., 2014). Also, Chanson et al. (2007) found that using TKE has the advantage of reducing error even with smaller number of data set than using Reynolds stress to understand flow mechanism in open channel flow. Thus, several investigators including Soulsby and Dyer (1981) and Stapleton and Huntley (1995) have explored TKE as a possible parameter in the shear stress estimation, but their studies were only conducted in a gradually-varied flow or one dimensional flow in the wave flume. Later, Dey and Lambert (2005) calculated bed shear stress by using several existing equations and found that TKE is the most suitable parameter that represents measured scour depth contours on sand bed. Recently, Kara et al. (2014) conducted computer simulation and also showed that bed shear stress distributions near the bridge has similar patterns with the TKE distributions. However, even if the TKE is proved as a good indicator that can be used to estimate bed shear stress, Dey and Lambert (2005) pointed out that the current value of experimental coefficient (=0.19) in Eq. (8) does not account for the effect of three dimensional, rapidly-varied flow where the flow contraction occur around an obstruction, and thus, proper laboratory experiment should be conducted to find the actual value of shear stress leading to the sediment transport, deposition, and channel change. Therefore, in this laboratory study, the complex three-dimensional flow field is reproduced by installing various widths of artificial structure and the effect of flow contraction and concomitant turbulent structures are explored in the laboratory. Then, the characteristics of shear stress around the structure is analyzed by using measured flow variables as well as turbulent quantities, and the results are used to re-formulate empirical coefficient for Eq. (8) suitable for the three-dimensional complex flow fields.

2 Methods

2.1 Experimental setup

The experiments were performed in a 15 m long and 1.5 m wide tilting laboratory flume at West Virginia University, USA. The channel slope (S_0) was set to 0.002 and the slope was categorized as a mild slope based on the comparison between normal depth and critical water depth calculations for all of the experimental conditions. Uniform plaid patterns were carved on top of the entire false floor surface to reproduce coarse-grained river-bed and to create fully rough turbulent flow through the entire flume. The corresponding roughness height generated by the pattern is about 3.5 mm. The water was recirculated from the large end tank to the upstream reservoir via two pumps with a maximum discharge of 0.095 m^3/s. An artificial shape of vertical structure was installed at 10 m downstream from the water entrance section and protruded from one side of flume. Three different widths of the obstruction structure, 0.23, 0.56 and 1.06 m, were used to simulate wide range of flow contraction and the corresponding turbulent structures that can be found in a field such as the flow between two rocks situated in a row or around an bridge abutment, but the streamwise length of the structure was kept in constant as 0.5 m. During the experiment, water depth was measured by using a point gauge ($\pm$0.1 mm) and point velocities as well as turbulent quantities were measured by using 3D-downlooking ADV. Where the higher turbulent flow is expected such as close to the structure, water depth as well as velocity/turbulent measurements were repeated several times to minimize measurement error.

ADV can measure three-dimensional velocity in the maximum response frequency of 50 Hz. Based on Nezu and Nakagawa (1993), the maximum response frequency is larger than 10 to 36 Hz to measure turbulent (SonTek, 2001). Measurements using ADV also require many samples to estimate the turbulent characteristics. In the study of Chanson et al. (2007), error on second statistical moments decreases as the number of sample increases. Thus, at least 9,000 sampling numbers, which is equal to 3 minutes with 50 Hz response frequency, were collected in each measurements for estimating the turbulent characteristics (Ge et al., 2005; Hong et al., 2015). After finishing each measurements by using ADV, post processing of the measured data was performed to remove the noise based on the protocols suggested by Nortek (1998), Sontek, (2001), and Hong et al. (2015) because noise occurs when a high level of turbulence exists at the measuring location. The first post processing protocol was to filter the measured time series data according to a minimum value of the correlation coefficient which is 70 percent for acceptance of data from each sampling period based on the recommendation of the ADV manufacturer for measurement of turbulence properties. The phase-space despiking algorithm of Goring and Nikora (2002) was also employed to remove any spikes in the time record caused by aliasing of the Doppler signal which sometimes occurs near a boundary. In addition to the required minimum correlation coefficient value and phase-space despiking algorithm, the signal-to-noise (SNR) was maintained at a value greater than 15 for accurate measurement of turbulence quantities.

2.2 Experimental procedure

In the beginning of each experiment, the desired discharge was set by main control panel. When the flow was stabilized in the flume, the required value of water depth was set by adjusting tail gate position. Then, as shown in Fig. 1, detailed measurements were conducted in the approach section which is located at 2.5 m upstream from the structure and in the test section where the obstruction structure was built. In the approach section, the point velocities and turbulent quantities were measured at 0.3~0.5 cm increments vertically close to the bed, but at the distance from the bed greater than 3 cm, measured at 1~2 cm increments vertically at the center of the approach cross-section. Within the test section, as shown in Fig. 1, total 5 cross sections were selected for water surface elevation, velocity and turbulent measurements. Along the each cross-section, water surface elevations were measured every 1cm laterally, and point velocities and corresponding turbulent quantities are measured at multiple vertical transects which are separated 3 to 5 cm laterally close to the obstruction structure, but 10 cm laterally at the region far from the structure where the effect of local flow contraction by flow acceleration and formation of shear layers is diminished. During the water depth measurements, additional measurements were made along the center of the flume to delineate water surface profile to find the slope of energy grade line through the entire test section and the flume.

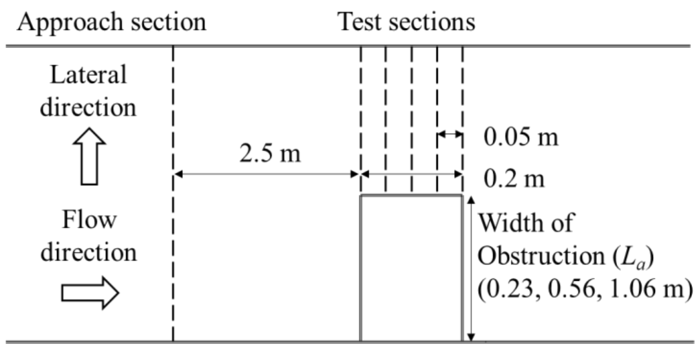

Figure 1. Schematic diagram of flow measurement points

3 Results

Total twelve flow conditions were simulated during the experiments to comprehensively address the purpose of this study. The experimental conditions have been summarized in Table 1, where, L_a: width of the obstruction, $\overline{u_1}$: mean velocity in the approach section, h_1: water depth in the approach section, q_2/q_1 or q_{2max}/q_1: flow contraction ratio, q_2: discharge per unit width in the test sections, q_1: discharge per unit width in the approach section, q_{2max}: maximum discharge per unit width in the test section, h_1/h_{n1}: dimensionless value representing backwater amount, h_{n1}: normal water depth in the approach section calculated by using manning's equation, S_1: water surface slope in the approach section. Here after, subscript "1" and "2" illustrate approach section and test section, respectively.

Fig. 2 shows the measured point velocities at the approach section for selected experimental cases. As shown in Fig. 2, the vertical distribution of measured velocity at the approach section was found to agree well with logarithmic velocity profiles in all experimental cases. Thus, depth-averaged mean velocity in the approach section ($\overline{u_1}$) in Table 1 was evaluated as the point velocity from the best-fit log relation at a relative distance above the bed of 0.4 times the depth (Sturm, 2010). However, in the test section, the depth-averaged velocities were calculated by taking the integral of the point velocity (u) measurements within each vertical profile over the depth and dividing by the water depth because the velocity profile within the test section did not have a logarithmic relationship due to its complex three-dimensional behavior induced by local flow contraction around the obstruction structure. Then, the value of discharge per unit width in the approach (q_1) and test section (q_2) was evaluated as the depth-averaged velocity times corresponding water depth at each point, and the maximum value of q_2 was selected as q_{2max} among the values of the discharge per unit width along the upstream face of the structure.

Table 1. *Experimental Conditions in this study*

Cases	L_a (m)	$\overline{u_1}$ (m/s)	h_1 (m)	Q_1 (m^3/s)	q_2/q_1	q_{2max}/q_1	h_1/h_{n1}	S_1
Case 1	0.23	0.432	0.1014	0.0657	1.251	1.326	1.216	0.0013
Case 2		0.453	0.1071	0.0728	1.226	1.293	1.205	0.0014
Case 3		0.473	0.1168	0.0828	1.250	1.322	1.212	0.0008
Case 4		0.509	0.1217	0.0929	1.229	1.284	1.175	0.0015
Case 5	0.56	0.365	0.1120	0.0613	1.582	1.626	1.404	0.0018
Case 6		0.378	0.1198	0.0680	1.591	1.670	1.406	0.0017
Case 7		0.375	0.1277	0.0719	1.607	1.697	1.448	0.0021
Case 8		0.384	0.1514	0.0871	1.666	1.745	1.522	0.0013
Case 9	1.06	0.143	0.1236	0.0265	3.323	3.602	2.601	0.0034
Case 10		0.170	0.1545	0.0394	3.203	3.334	2.546	0.0034
Case 11		0.182	0.2176	0.0595	3.257	4.184	2.776	0.0026
Case 12		0.205	0.2200	0.0675	3.281	3.983	2.594	0.0027

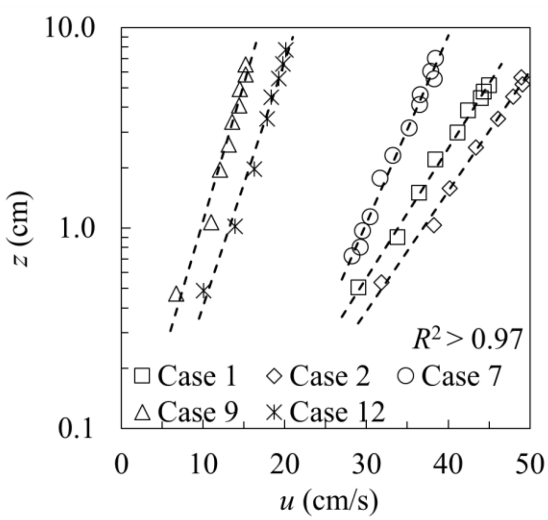

Figure 2. Vertical velocity profiles in the approach section.

In order to determine the reliability of the measured data, discharge in the approach section (Q_1) and the test section (Q_2) was calculated with the measured value of velocities and water depths, and continuity check was evaluated between them. As shown in Fig. 3, the results show good agreement (R^2 = 0.97 and Root mean square error (RMSE)= 0.03).

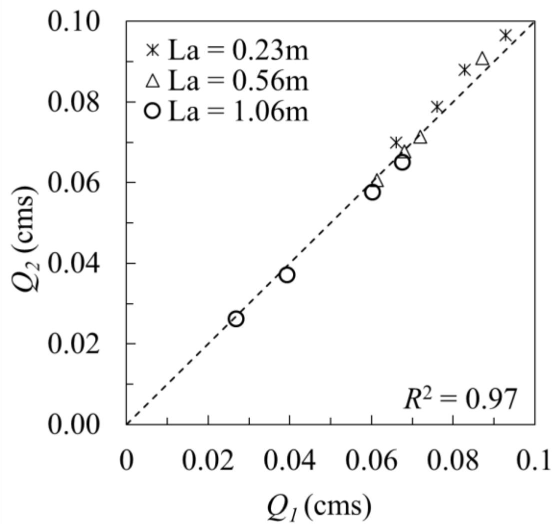

Figure 3. Continuity between the approach and the test section; where, Q_1 and Q_2 is discharge in the approach and test section, respectively.

Turbulent quantities near the bed is an important variable to account for the impact of the local turbulence energy generated by the vortex structure and the separated shear zone on bed shear stress leading to local erosion and deposition (Ge et al., 2005; Lacey & Rennie, 2012). Furthermore, based on the Launder and Rodi (1983)'s findings in wall jet flow , the maximum value of velocity fluctuation occurs near the wall. Thus, to quantify the local turbulence effect on the shear stress, turbulent quantities were measured at a height of 5 mm above the bed and used for the further analysis because 5 mm is the closest point that the ADV can measure. At the height of 5 mm from the bed, the value of z^+(dimensionless depth; zu_*/ν) is from 50 to 80 in this experiment, where is theoretically considered as the outer layer ($z^+ > 30$) (Sturm, 2010), and the maximum value of turbulent quantities including Reynolds stress and TKE are found (Hong et al., 2015).

3.1 Flow characteristics

The flow constriction through the test section by the existence of the obstruction structure gives rise to both contraction and expansion energy losses, with a resulting rise in water surface elevation at the approach section in comparison to that which would occur without the flow constriction. The measured water surface profiles along a centerline of the entire flume from the approach to the test section in this study proves the back-water scenario caused by the energy losses. Effect of the back water can be estimated by the flow contraction ratio between approach section and the test section (q_2/q_1) (Hong et al., 2015). Thus, to find the effect of backwater in the approach section in this experiment, the dimensionless value representing backwater amount (h_1/h_{n1}) are plotted with the value of (q_2/q_1) in Fig. 4 (a). As shown in Fig. 4 (a), as the flow contraction ratio (q_2/q_1) increases in *x*-axis, the value of h_1/h_{n1} also increases, accordingly. As the width of the obstruction structure increases, the value of q_2/q_1 increases due to higher flow acceleration through the test section and resulting larger contraction and expansion losses through the test section lead to larger effect of back water in the approach section. The results clearly reveal that the back-water effect can be considered as direct function of flow contraction ratio as suggested by Hong et al. (2015) and the findings will be used in the following section to explore the effect of back water on the bed shear stress in the approach section.

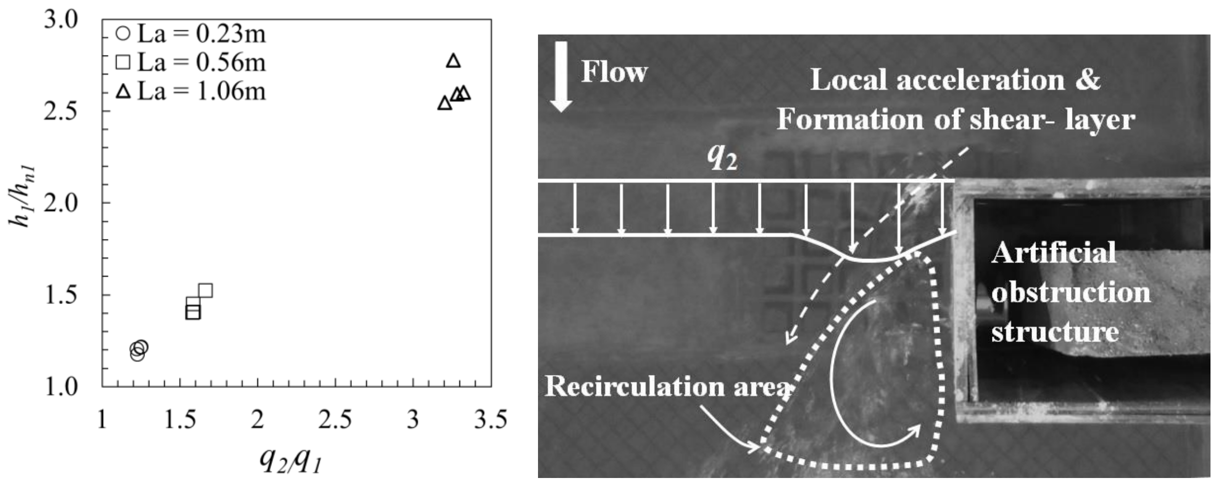

(a) (b)

Figure 4. (a) Back water effect in the approach section and (b) flow characteristic in the test section.

As shown in Table 1, the slope of water surface profile in the approach section (S_1) for several cases is slightly larger than channel bed slope (S_0 = 0.002). Based on the findings by Chow (1959), gradually-varied flow in a prismatic channel can be defined as the water surface slope is within $\pm S_0$. Thus, flow regime in the approach section for several cases cannot be categorized as gradually-varied flow. In the test section, as shown in the Fig. 4 (b), it is obvious that the flow conditions are rapidly-varied flow because local flow acceleration around the obstruction resulted in three-dimensional complex flow patterns through the entire test section. Fig. 4 (b) clearly depict the unsteady roll up of the shear layer near the corner of structure where the local flow contraction is greatest and the formation and shedding of eddies and the transport of these eddied downstream within re-circulation area where the estimation of shear stress is tricky due to the complex flow patterns. Fig. 4 (b) also shows the lateral distributions of discharge per unit width (q_2) along the entrance of the test section. As shown in the q_2 distribution, the maximum value of discharge per unit width (q_{2max}) is observed near the corner of the obstruction where the dominant shear layer start to occur and extend through the constriction section along the boundary of re-circulation area. The effect of the flow contraction through the test section on the bed shear stress will be explained in more detail in the next section.

3.2 Bed shear stress in the approach section

As explained in the previous paragraph, the flow regime in the approach section was not uniform flow because of the back-water effect. Thus, to find the effect of back water on shear stress calculated by using various formulas in the approach section, bed shear stress estimated by all four equations is compared with flow contraction ratio (q_2/q_1) which is a representative parameter of backwater. Fig. 5 shows the comparison results. As shown in Fig. 5, as the value of q_2/q_1 increase in *x*-axis, the bed shear stress decrease because effect of the back water becomes higher as q_2/q_1 increase, and the resulting upstream approach depth is larger than the normal depth for the case without flow constriction under the same discharge. Even if the calculated shear stress seems to follow the similar decreasing trend with respect to the value of q_2/q_1 with all four methods, the results from Eq. (1) (water depth) and Eq. (3) (shear velocity) shows larger value than the results using Eq. (7) (Reynolds stress) and Eq. (8) (TKE), but, both of equations using the local turbulent quantities (Eq. (7) (Reynolds stress) and Eq. (8) (TKE)) shows similar magnitude of the shear stress. The larger outcome from Eq.(1) and Eq. (3) is because they cannot correctly account for the bed coarseness effect as in this study and also, they are based on the simplified assumption such as under uniform flow condition and gradually-varied flow condition, respectively. Also, Nezu and Nakagawa (1993), Biron et al. (2004), and Rowinski et al. (2005) explored that Eq. (1) and Eq. (3) is considered inappropriate for the cases with back water conditions.

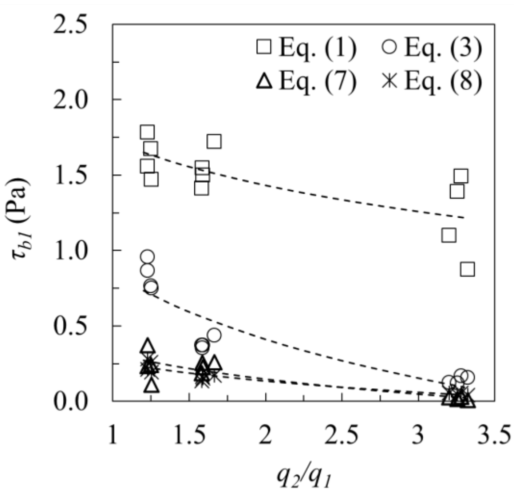

Figure 5. Effect of back water on the bed shear stress in the approach section

As shown in Fig. 5, even if both of the Eq. (7) and Eq. (8) shows similar results in the approach section, under the complex three-dimensional flow conditions through the test section, Mathieu and Scott (2000) suggested that using Reynolds stress is often considered as the most appropriate tool for evaluation of the bed shear stress because the empirical coefficient in Eq. (8) should be re-visited to correctly account for complex non-uniformity. Thus, the results using Eq. (7) was used for the reference bed shear stress for further analysis, and in the following chapter, bed shear stress calculated by using TKE (Eq. (8)) is compared with that from Reynolds stress to suggest surrogate method of shear stress estimation using TKE, because as explained in the previous paragraph, TKE is also one of the most suitable parameter representing bed shear stress with respect to their error amount in measurements and calculations, but a new empirical coefficient suitable for complex three dimensional flow filed should be suggested for its use.

3.3 Bed shear stress in the test section

Because of their simplified assumption in Eq. (1) and Eq. (3), bed shear stress within the test section can only be estimated by using Eq. (7) and Eq. (8), and Fig. 6 shows the spatial distribution of bed shear stress within the test section around the obstruction structure estimated by using Eq. (7) and Eq. (8), respectively. In Fig. 6, the origin of *x* (streamwise direction) and *y* (lateral direction) is located at the upstream corner of the obstruction structure. As shown in Fig. 6, both of formulas resulted in similar patterns of the bed shear stress distribution in which largest bed shear stress is located near the upstream corner of the structure where highly three-dimensional flow is characterized by local flow acceleration and the resulting shear layer starting to develop at the corner of the structure and extending along the tangent of re-circulation area where large-scale unsteadiness is found. When the flow area is reduced by bankline abutments on both side of a narrow main channel in a river, flow accelerates through the contraction between the abutment, and the higher velocity is responsible for the higher shear stress. In addition to the higher velocity due to the mean flow acceleration, local turbulent flow structures, such as the horseshoe and tornado-like vortices resulting from flow separation on the upstream corner of the abutment and re-circulation zone behind the shear layer have been responsible for the additional magnitude of the shear stress close to the abutment. (Hong & Irfan, 2019). The results shown in Fig. 6 is corresponding to the previous studies conducted by Dey et. al. (2005) and Duan (2009). Their studies show that maximum Reynolds stress and maximum TKE were found around the corner of the structure where large vortex structure occurs near the shear layer.

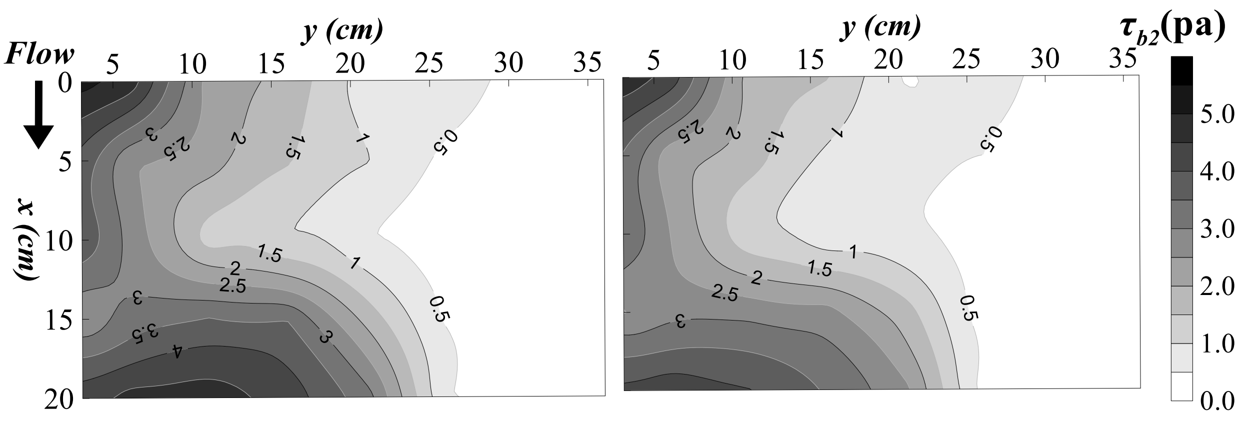

Figure 6. Spatial distribution of bed shear stress within the test section for case 7 estimated by Eq. (7) in (a) and Eq. (8) in (b)

However, as shown in Fig. 6 (a) and (b), the absolute value of bed shear stress from those two different formulas are different. Similar results were found in other researches (Biron et al., 2004; Dey & Lambert, 2005; Duan, 2009; Kara et al., 2014; Lee, 2019;Yaeger, 2009) that the bed shear stress estimation using TKE shows lower than that from Reynolds stress around the bridge abutment when the Eq. (8) was applied. The most probable reason is that the empirical coefficient (C_{exp} = 0.19) in Eq. (8) is based on the gradually-varied flow in oceanography studies (Soulsby & Dyer, 1981; Stapleton & Huntley, 1995) which cannot account for the effect of complexity as in this study, thus, the experimental coefficient should be re-evaluated.

Additional proof for the reason of updating empirical coefficient in Eq. (8) shows in Fig. 7. Experimental results from the current study was compared with Biron et al. (2004) and Yaeger (2009) in Fig. 7, where *x*-axis is the shear stress estimated by Eq. (7), but *y*-axis shows the value estimated by Eq.(8). Biron et al. (2004) installed a 0.05 m wide of deflector within a 0.4 m wide flume to generate short contraction (L_a/W = 0.125, in which W is width of the flume) and run the experiment under the low flow rates. Based on the experiment, they also calculate/estimate shear stress around the deflector using same formulas as in this study and the results are included in Fig. 7. Yaeger (2009) also conducted similar experiment, but instead of using one flow obstruction structure, a series of three deflecting dikes (L_a/W = 0.267) were installed perpendicular to the flow direction to find the effect of dike placement on the turbulence flow fields. As shown in Fig. 7, values of shear stress including Biron et al. (2004) and Yaeger (2009) follows one to one line in lower bound of *x*-axis. However, as the value of shear stress increases in *x*-axis, the comparison shows bias instead of aggregating them into the one to one single line. When the flow contraction becomes higher, the corresponding value of shear stress through the contraction also becomes larger because of the complex flow fields associated with flow accelerations and resulting local turbulent structures along a shear layer. However, as already explained in the previous paragraph, the empirical coefficient (C_{exp}= 0.19) in Eq. (8) was decided based on the simple one-dimensional flow types and thus, leading to underestimation of the shear stress compared to the formula using Reynolds stress in three dimensional complex flow. Furthermore, the constant value of empirical coefficient is not suitable to address the complexities around the obstruction such as a rock or a abutment in this study, deflector (Biron et al., 2004), and dikes (Yaeger, 2009); instead, the empirical coefficient should be function of amount of energy generated by turbulent structure which varies with the flow contraction ratio (Lee and Hong 2019). It is interesting to note that the lower bound of shear stress using Eq. (8) is about - 80% of that using Eq. (7). It is obscure to explore the qualitative answers in this study, thus, additional laboratory experiment and/or numerical simulations should be conducted.

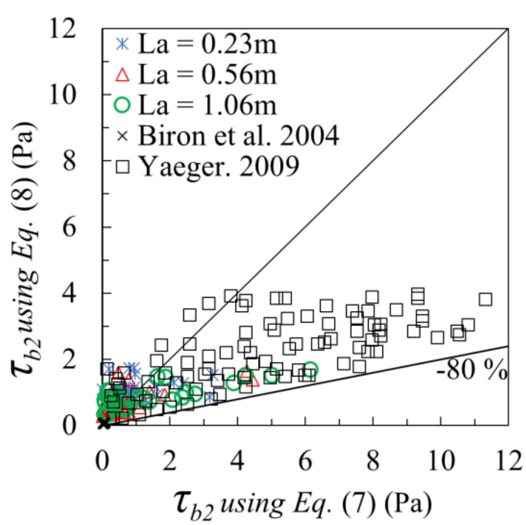

Figure 7. Comparison of bed shear stress calculated by using Eq. (7) and Eq, (8) including Biron et al. (2004) and Yaeger (2009); where, τ_{b2}: bed shear stress in the test section.

4 Analysis and Discussion

As explored by many other researchers, the maximum value of bed shear stress is mainly located near the upstream corner of an instream structure when the structure obstructed the flow area. Usually, an instream structure remained intact during the flow movement, and the maximum amount of sediment/material's transport occurred around the upstream corner of the structure where the local flow contraction is maximum, and power of turbulent vortex structure is concentrated. The similar explanation can be found in Fig. 6 in this study. Furthermore, in the engineering viewpoint, the location is important to forecast the vulnerability of hydraulic infrastructures because the maximum bed shear stress lead to foundation exposure during the high-water mark. Thus, in this study, the region where the maximum shear stress is found was selected for additional analysis of bed shear stress, and the analysis and discussions are shown below.

4.1 Dimensionless bed shear stress

The effects of flow contraction as well as local turbulence, all contribute to the maximum shear stress around the obstruction. Between those two main drivers, the effect of local turbulence can be parametrized by flow contraction ratio (q_2/q_1), the ratio of discharge per unit width through the test section to that in the approach flow (Hong et al., 2015). As a result, it can be hypothesized that the maximum shear stress around the obstruction structure is related to the value of flow contraction ratio only. Thus, as an initial fit, the maximum shear stress normalized by the shear stress in the approach section are plotted in Fig. 8 (a) according to the value of q_2/q_1.

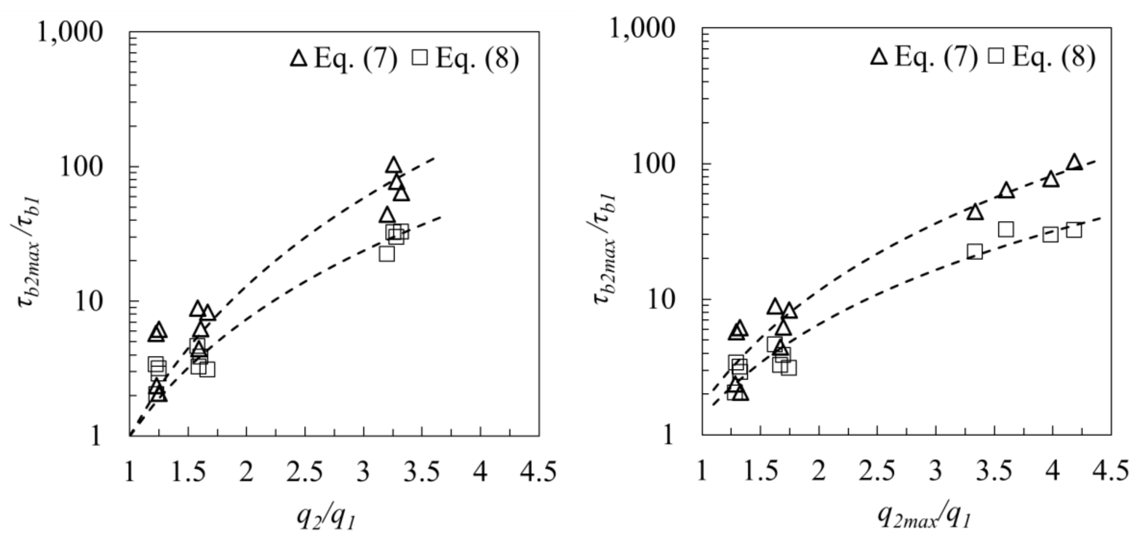

(a) (b)

Figure 8. Normalized maximum shear stress around the corner of the rock , τ_{b2max}/τ_{b1}, as a function of q_2/q_1 in a) and $q_{2\max}/q_1$ in b).

As shown in Fig. 8 (a), as the flow contraction ratio (q_2/q_1) in the *x*-axis increases, normalized maximum shear stress, τ_{b2max}/τ_{b1}, calculated by using both formulas gradually increases in semi-logarithmic scale. Even though the observed data shows similar power relationships in both cases, the case with TKE shows lower value than the case with Reynolds stress because improper value of empirical coefficient in Eq. (8) was used for the calculation. To find the best-fit equation, a least-squares regression analysis was conducted on the data given in Fig. 8(a). Physically, as the value of q_2/q_1 approaches to 1, the effect of flow contraction becomes smaller and finally the value of τ_{b2max}/τ_{b1} becomes unity. Thus, during the least-squares analysis, the best-fit equation is forced to pass through the origin and the formulas are shown as follows,

$$\frac{\tau_{b2max}}{\tau_{b1}} = \left(\frac{q_2}{q_1}\right)^{3.703} \qquad \text{Eq. (9a)}$$

$$\frac{\tau_{b2max}}{\tau_{b1}} = \left(\frac{q_2}{q_1}\right)^{2.833} \qquad \text{Eq. (9b)}$$

with coefficient of determination of 0.86 and 0.91, respectively. Eq. (9a) and Eq. (9b) is best-fit equation for using Reynolds stress and TKE, respectively. As shown in the regression analysis, the exponent of Eq. (9a) is larger than Eq. (9b), but both Eq. (9a) and Eq (9b) state that maximum dimensionless shear stress is function of mean discharge contraction ratio.

However, this preliminary result is oversimplified because in terms of limiting cases, when a rock and/or an instream structure is located within a wide river, the value of q_2/q_1 is close to 1. But, still higher value of shear stress around the corner is there that is driven by the dynamics of the horseshoe vortex (Koken & Constantinescu, 2009) alone. Thus, the mean value of discharge contraction ratio are not necessarily expected to be a good indicator over a larger range of the independent variables as limiting cases are approached because the relative effect of turbulence will be different depending on the size of obstruction, the approach flow velocity distribution, and many other factors. Under these circumstances, parameterizing the role of turbulence through its structure (oscillating horseshoe vortex, increased vorticity due to the horse shoe vortex and separated shear flow) seems to be a formidable task. However, at the most basic level, it is hypothesized that the contribution of local turbulence in the vicinity of the obstruction is elevated local velocity close to the structure that provides the additional energy to the bed. Based on the similar understanding, Sturm (1999) and Hong (2013) suggested possibility to use the maximum depth-averaged velocity, $\overline{u_{2max}}$, near the corner of instream structure to estimate the amount of maximum sediment transport around the structure. Earlier, Biglari and Sturm (1998) developed a 2D, depth-averaged k -$\mathcal{E}$ turbulence model to determine the flow field around a setback abutment founded on the floodplain within a compound shape river and showed that the results from the numerical simulation for $\overline{u_{2max}}$, had good agreement with experimental maximum scour depth around the obstruction structure.

Thus, the lateral profile of discharge per unit width (q_2) (see the example of the profile in Fig. 4(b)) is observed along the upstream face of the structure and the maximum value ($q_{2max} = \overline{u_{2max}} h_2$) was selected among them where the flow contraction is the greatest and a strong shear layer related to the higher-velocity occurred. Table 1 shows the value of (q_{2max}/q_1) for each experimental case, and the data given in the table together with the normalized maximum shear stress in Fig. 8(b) were used to conduct another regression analysis as follows,

$$\frac{\tau_{b2max}}{\tau_{b1}} = 1.638\left(\frac{q_2}{q_1}\right)^{2.817} \qquad \text{Eq. (10a)}$$

$$\frac{\tau_{b2max}}{\tau_{b1}} = 1.350\left(\frac{q_2}{q_1}\right)^{2.275} \qquad \text{Eq. (10b)}$$

which, for this relationship, yields the coefficient of determination of 0.94 and 0.96 for the case with using Reynolds stress in Eq. (10a) and TKE in Eq. (10b), respectively. The relationships from the best-fit regression analysis given by Eq. (10) results in an increase in the value of the coefficient of determination from 0.86 to 0.94 and from 0.91 to 0.96 compared to Eq. (9), which confirms that q_{2max}/q_1 can be a better representative parameter for normalized shear stress estimation.

4.2 Revisting empiricical coefficient for bed shear stress estimation using TKE

As shown in Fig. 8, the normalized maximum shear stress estimated by using two different formulas followed a similar trend. Thus, setting the shear stress values from using Reynold stress as reference and by comparing the difference between two regression formulas in Eq. (9) and Eq. (10), Fig. 9 shows the empirical coefficient with respect to the value of q_2/q_1 and q_{2max}/q_1, respectively.

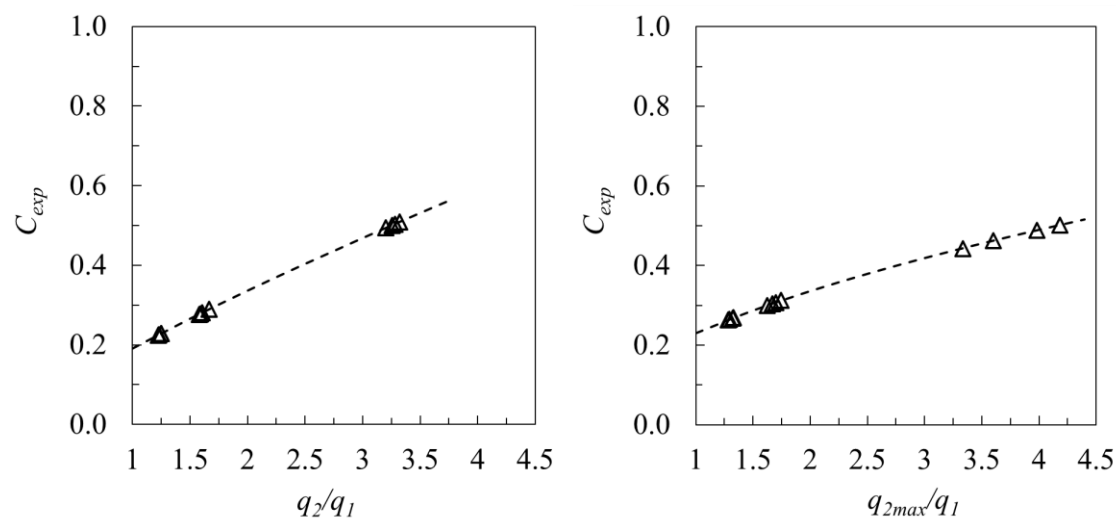

(a) (b)

Figure 9. Empirical coefficient for shear stress equation using TKE according to the flow contraction ratio, q_2/q_1 in (a) and q_{2max}/q_1 in (b).

and the empirical coefficient for three dimensional complex fields was suggested as follows,

$$C_{exp} = 0.19\left(\frac{q_2}{q_1}\right)^{0.82} \qquad \text{Eq. (11)}$$

$$C_{exp} = 0.231\left(\frac{q_{2max}}{q_1}\right)^{0.542} \qquad \text{Eq. (12)}$$

As shown in Fig. 9 and the Eq. (11) and (12), empirical coefficient is not a constant value under three dimensional complex flow, instead it shows unique function of flow contraction ratio because the empirical coefficient is a parameter accounting for the local turbulence effect in the vicinity of the obstruction structure, and the amount of turbulence effect is related to the degree of flow contraction between the approach and the test section. Furthermore, Eq. (12) state that the effect of turbulence alone under the limiting cases without any mean flow contraction should be 0.231 which shows higher constant compared 0.19 in Eq. (11) due to the flow complexity. For this relationship, the value of shear stress was re-calculated with newly suggested empirical coefficient in Eq. (12), then, similarity of the maximum bed shear stress between the case with Reynolds stress and case with TKE are shown in Fig. 10. As shown in Fig. 10, the bias becomes better because of applying the modified empirical coefficient for the calculation of maximum shear stress using TKE, and slope of regression line increased from 0.36 to 0.83 and R^2 of each regression line increased from 0.67 to 0.92.

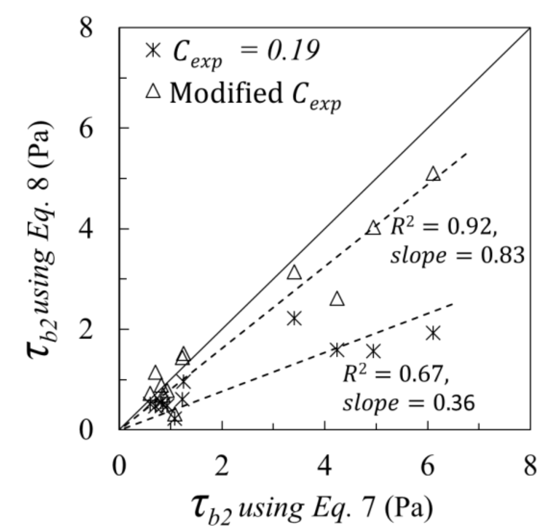

Figure 10. Correlation of maximum shear stress calculated by using constant empirical coefficient ($C_{exp} = 0.19$) and Eq. (12).

As explained in the previous section, q_{2max}/q_1 is better indicator. When the smaller value of q_2/q_1 (≈ 1) in the field where the size of obstruction structure is relatively small compared to a wide channel, only the turbulence structure is dominant driver causing higher shear stress. However, for practical purposes, quantifying $\overline{u_{2max}}$ in the field or even in the lab is challenging because the local turbulence varies depending on the obstruction structure's shape, the bed material, the flow types, and other factors. Therefore, based on the findings of this study, Eq. (11) also can be as a compromise.

5 Conclusions

Comparing critical shear stress for the initiation of motion with shear stress induced by flowing water in a river is important and preliminary task for scientist as well as engineers who are interested in the issue of sedimentation including erosion, transportation, and deposition. Thus, several shear stress formulas have been suggested in terms of various variables; among them, both of Reynolds stress and TKE are considered as the most suitable parameter that can be applied to calculate bed shear stress. However, the current version of methods using TKE has limitations under complex fields because it has been only verified in gradually-varied and uniform flow even though TKE has potential being a champion with respect to the amount of measurements error compared to the Reynolds Stress. Therefore, in this study, to improve the shear stress method using TKE, laboratory experiments were conducted in a tilting flume. The experimental results show that current version of TKE method underestimate the shear stress compared to that from Reynolds stress under three-dimensional complex flow fields, calling for calibrating the empirical coefficient. Therefore, based on the findings, newly formulated empirical coefficient for TKE methods was suggested with respect to the flow contraction ratio and the results shows good agreements with the shear stress calculated by using Reynolds stress.

It is expected that TKE will be of great help in studying bed shear stress. To make more solid connection between TKE and bed shear stress, more laboratory studies should be conducted, especially with using various shape of obstruction structure and over a wider range of q_{2max}/q_1 and/or q_2/q_1 including their range of ~1. Furthermore, with using LSPIV and/or PIV, more detailed velocity/turbulent measurements within recirculation area behind of the rock should be measured to confirm the relationship suggested in this study. In addition to the laboratory studies, A well-planned, detailed field study including real-time sedimentation monitoring between/around obstruction during normal and extreme hydrologic condition is required for the verification of the method developed in this study. Finally, a three-dimensional numerical model with advanced turbulence schemes should be applied to the laboratory model used in this study for their validations, and then wider range of flow conditions than covering by laboratory studies alone can be obtained in the area of research.

Acknowledgments

This research is supported by start-up of Dr.Seung Ho Hong from West Virginia University. We would like to show our thanks to Dr. Leslie Hopkinson and Dr. Omar I Abdul-Aziz in West Virginia University for reviewing and commenting on this work. The authors declare no conflict of interest.

Data availability statement

Datasets for this research are include in the master's thesis: Lee, J. S. (2019). Shear stress estimates in the approach and bridge section by using various formula., Master thesis, Retrieved from the research repository @ WVU (https://researchrepository.wvu.edu/etd/3791/). Morgantown WV, USA.

References

Ahmed, F., and Rajaratnam, N. (1998). "Flow around bridge piers." *Journal of Hydraulic Engineering*, 124(3), 288.

Biglari, B. and Sturm. T.W. (1998). "Numerical modeling of flow around bridge abutments in compound channel", *Journal of Hydraulic Engineering*, 124(2), 156-164.

Biron, P. M., C. Robson, M. F. Lapointe, and Gaskin, S. J. (2004), "Comparing different methods of bed shear stress estimates in simple and complex flow fields", *Earth Surface Processes and Landforms*, 29(11), 1403-1415.

Bouteiller, C.L. and Venditti, J.G. (2015). "Sediment transport and shear stress partitioning in vegetated flow.", *Water Resources Research*, 54(4), 2901-2922.

Buscombe, D. and Conley, D.C. (2012). "Effective shear stress of graded sediments." *Water Resources Research*, 48(5), 1-13.

Cardoso, A. H., Graf, W. H., and Gust, G. (1991). "Steady gradually accelerating flow in a smooth open channel." *Journal of Hydraulic Research*, 29(4), 525–543.

Chanson, H., Trevethan, M., and Koch, C. (2007). "Discussion of 'Turbulence measurements with acoustic Doppler velocimeters' by Carlos M. García, Mariano I. Cantero, Yarko Niño, and Marcelo H. García." *Journal of Hydraulic Engineering*, 133(11), 1283–1286.

Cheng, N., Tang, C., and Zhu, L. (2004). "Evaluation of bed load transport subject to high shear stress fluctuations." *Water Resources Research*, 40(5), 1-5.

Choo, H., Zhao, Q., Burns, S., Sturm, T., and Hong, S. (2020). "Laboratory and theoretical evaluation of impact of packing density, particle shape, and uniformity coefficient on erodibility of coarse-grained soil particles." *Earth Surface Professes and Landforms*., 45(7), 1499-1509.

Chow, V. T. (1959). Open channel hydraulics, McGraw-Hill, New York.

Dey, S., and Barbhuiya, A. K. (2005). "Flow field at a vertical-wall abutment.", *Journal of Hydraulic Engineering*, 131(12), 1126-1135.

Dey, S., and Lambert, M. F. (2005). "Reynolds stress and bed shear in nonuniform unsteady open channel flow.", *Journal of Hydraulic Engineering*, 131(7), 610-614.

Duan, J. G. (2009). "Mean flow and turbulence around a laboratory spur dike.", *Journal of Hydraulic Engineering*, 135(10), 803-811.

Einstein, H.A. (1942). "Formulas for the transportation of bed load.", *Transactions* [ASCE], 2140(107), 561-573.

Etminan V., Ghisalberti, M., and Lowe, R. (2018). "Predicting bed shear stresses in vegetated channels.", *Water Resources Research*, 54(11), 9187-9206.

Galperin, B., Kantha, L. H., Hassid, S., and Rosati, A. (1988). "A quasi-equilibrium turbulent energy model for geophysical flows.", *Journal of the Atmospheric Sciences*, 45(1), 55-62.

Ge, L., Lee, S., Sotiropoulos, F., and Sturm, T. W. (2005). "3D unsteady RANS modeling of complex hydraulic engineering flows. Part II: Model validation and flow physics", *Journal of Hydraulic Engineering*, 131(9), 809-820.

Goring, D. and Nikora, V. (2002). "Despiking acoustic Doppler velocimeter data", *Journal of Hydraulic Engineering*, 128(1), 117-126.

Hong, S. (2013). *Prediction of clear-water abutment scour depth in compound channel for extreme hydrologic events*. PhD thesis, Retrieved from Smartech Home @ Georgia Tech (https://smartech.gatech.edu/handle/1853/47535?show=full). Atlanta, GA, USA.

Hong, S., Sturm, T, and Stoesser, T. (2015). "Clear water abutment scour in a compound channel for extreme hydrologic events." *Journal of Hydraulic Engineering*, 141(6), 1-12.

Hong, S., and Lee, S. O. (2018). "Insight of Bridge Scour during Extreme Hydrologic Events by Laboratory Model Studies". *KSCE Journal of Civil Engineering*, 22(8), 2871-2879.

Hong, S. and Abid, I. (2019). "Scour around an erodible abutment with riprap apron over time." *Journal of Hydraulic Engineering*, 145(6), 1-6.

Jeon, J., Lee, J., and Kang, S. (2018). "Experimental investigation of three-dimensional flow structure and turbulent flow mechanisms around a nonsubmerged spur dike with a low length-to-depth ratio." *Water Resources Research*. 54(5), 3530-3556.

Johnson, E. and Cowen, E. (2017). "Estimating bed shear stress from remotely measured surface turbulent dissipation fields in open channel flows." *Water Resources Research*. 53(3), 1982-1996.

Kang, S., Hill, C., and Sotiropoulos, F. (2016). "On the turbulent flow structure around an instream structure with realistic geometry." *Water Resources Research*. 52(10), 7869-7891.

Kara, S., Stoesser, T. Sturm, T.W. and Mulahasan, S. (2014). "Flow dynamics through a submerged bridge opening with overtopping." *Journal of Hydraulic Research*, 53(2), 186-195.

Kironoto, B. A., and Graf, W. H. (1995). "Turbulence characteristics in rough Nonuniform open-channel flow.", *Proceedings of the institution of civil engineers-water maritime and energy*, 112(4), 336-348.

Knight, D.W. and Demetriou, J.D. (1983). "Floodplain and main channel flow interaction." *Journal of Hydraulic Engineering*, 109(8), 1073-1092.

Koken, M. and Constantinescu, G. (2009). "An investigation of the dynamics of coherent structures in a turbulent channel flow with a vertical sidewall obstruction." *Phys. Fluids*, 21(8), ,085104.

Kundu, P., Cohen, Ira., and Dowling, D. (2015). Fluid Mechanics, 6th edition, Academic Press.

Lacey, R.W. Jay and Rennie, C.D. (2012). "Laboratory investigation of Turbulent flow structure around a bed-mounted cube at multiple flow stages", *Journal of Hydraulic Engineering*, 138(1), 71-84.

Landers, M., and Sturm, T. (2013). "Hysteresis in suspended sediment to turbidity relations due to changing particle size distributions." *Water Resources Research*. 49(9), 5487-5500.

Launder, B. E., and Rodi, W. (1983). "The turbulent wall jet measurements and modeling.", *Annual Review of Fluid Mechanics*, 15(1), 429-459.

Lee, J. S. (2019). *Shear stress estimates in the approach and bridge section by using various formula*., Master thesis, Retrieved from The research Repository @ WVU (https://researchrepository.wvu.edu/etd/3791/). Morgantown, WV, USA.

Lee, S.O. and Hong, S. (2019). “Turbulence characteristics before and after scour upstream of a scaled-down bridge pier model”. *WATER*, 11, 1900, 1-14.

Lefebvre, A., Paarlberg, A., and Winter, C. (2014). “Flow separation and shear stress over angle-of-repose bed forms: A numerical investigation.” *Water Resources Research*. 5(2), 986-1005.

Ligrani, P. M., and Moffat, R. J. (1986). “Structure of transitionally rough and fully rough turbulent boundary layers.”, *Journal of Fluid Mechanics*, 162, 69-98.

Mathieu, J., and Scott, J. (2000). An introduction to turbulent flow. Cambridge University Press.

Monsalve A., and Yager, E. (2017). “Bed surface adjustments to spatially variable flow in low relative submergence regimes.” *Water Resources Research*. 53(11), 9350-9367.

Monteith, H., and Pender, G. (2005). “Flume investigations into the influence of shear stress history on a graded sediment bed.” *Water Resources Research*. 41(12), 1-8.

Myers, R.C. (1978). “Momentum transfer in a compound channel.” *Journal of Hydraulic Research*, 16(2), 139-150.

Myers, R.C. and Lyness, J.F. (1997). “Discharge ratios in smooth and rough compound channels.” *Journal of Hydraulic Engineering*, 123(3), 182-188.

Mueller, E., Pitlick, J., and Nelson, J.M. (2005). “Variation in the reference Shields stress for bed load transport in gravel-bed streams and rivers.” *Water Resources Research*. 41(4), 1-10.

Nezu, I., Kadota, A., and Nakagawa, H. (1997). “Turbulent structure in unsteady depth-varying open-channel flows.” *Journal of Hydraulic Engineering*, 123(9), 752–763.

Nezu, I., and Nakagawa, H. (1993). Turbulence in open channels. IAHR/AIRH Monograph. Balkema, Rotterdam, The Netherlands.

Nezu, I., and Rodi, W. (1986). “Open-channel flow measurements with a laser Doppler anemometer.”, *Journal of Hydraulic Engineering*, 112(5), 335-355.

Nortek, A. S. (1998). ADV operation manual. Vollen, Norway, 34.

Parker, G. and Klingeman, P. (1982). “On why gravel bed streams are paved.” *Water Resources Research*. 18(5), 1409-1423.

Petit, F. (1987). “The relationship between shear stress and the shaping of the bed of a pebble-loaded river larulles-Ardenne.”, *CATENA*, 14(5), 453-468.

Rankin, K. L., and Hires, R. I. (2000). “Laboratory measurement of bottom shear stress on a movable bed.”, *Journal of Geophysical Research: Oceans*, 105(C7), 17011-17019.

Rowiński, P., Aberle, J., and Mazurczyk, A. (2005). “Shear velocity estimation in hydraulic research.”, *Acta Geophysica Polonica*, 53(4), 567-583.

Shamloo, H., Rajaratnam, N., and Katopodis, C. (2001). “Hydraulics of simple habitat structures.”, *Journal of Hydraulic Research*, 39(4), 351-366.

Shiono, K. and Knight, D.W. (1991). “Turbulent open-channel flows with variable depth across the channel.” *Journal of Fluid Mechanics*, 222, 617-646

Shields, A. (1936). “Application of similarity principles and turbulence research to bed-load Movement.”, W.P. ott and J.C. van Uchelen. Hydrodynamics Laboratory Publ. No. 167. Pasadena, California Institute of Technology.

Shvidchenko, A., Pender, G., and Hoey, T. (2001). “Critical shear stress for incipient motion of sand/gravel streambeds.” *Water Resources Research*. 37(8), 2273-2283.

Sime, L., Ferguson, R., Church, M. (2007). “Estimating shear stress from moving boat acoustic doppler velocity measurements in a large gravel bed river.” *Water Resources Research*. 43(3), 1-12.

Smart, G. M. (1999). “Turbulent velocity profiles and boundary shear in gravel bed rivers.”, *Journal of Hydraulic Engineering*, 125(2), 106-116.

Song, T., and Chiew, Y. M. (2001). “Turbulence measurement in nonuniform open-channel flow using acoustic Doppler velocimeter (ADV).”, *Journal of Engineering Mechanics*, 127(3), 219-232.

SonTek (2001). Acoustic Doppler Velocimeter (ADV) principles of operation, SonTek Technical Notes, SonTek, San Diego, CA.

Soulsby, R.L. and Dyer K.R. (1981) “The form of the near-bed velocity profile in a tidally accelerating flow.”, *Journal of Geophysical Research*, 86 (9) (1981), 8067-8074

Stapleton, K. R., and Huntley, D. A. (1995). “Seabed stress determinations using the inertial dissipation method and the turbulent kinetic energy method.”, *Earth surface processes and landforms*, 20(9), 807-815.

Sturm T.W. (1999). “Abutment scour studies for compound channels”, Washington, DC, Federal Highway Administration, U.S. Department of Transportation Report No. FHWA-RD-99-156.

Sturm T. W. (2010). Open channel hydraulics, McGraw-Hill, New York.

Sukhodolov, A (2012). “Structure of turbulent flow in a meander bend of a lowland river.” *Water Resources Research*. 48(1), 1-21.

Tu, H., and Graf, W. H. (1993). “Friction in unsteady open-channel flow over gravel beds.” *Journal of Hydraulic Research*, 31(1), 99–110.

Wilcock, P. (1996). “Estimating local bed shear stress from velocity observations.” *Water Resources Research*. 32(11), 3361-3366.

Wormleaton, P.R. and Hadjipanos, P. (1985). “Flow distribution in compound channels.” *Journal of Hydraulic Engineering*, 111(2), 357-361.

Yang, S. Q. (2005). “Formula for sediment transport in rivers, estuaries and coastal waters.” *Journal of Hydraulic Engineering*, 131 (11): 968–979

Yaeger M.A. (2009). *Mean flow and turbulence around two series of experimental dikes*, Master’s thesis, Retrieved from Repository @ the university of Arizona (https://repository.arizona.edu/handle/10150/193453). Tucson, AZ, USA.

Yang J., Kerger, F., and Nepf, H. (2015). “Estimation of the bed shear stress in vegetated and bare channels with smooth beds.”, *Water Resource Research*, 51(5), 3647-3663.